NATIONAL ADVISORY COMMITTEE FOR AERONAUTICS

TECHNICAL NOTE

No. 1308

ISOLATED AND CASCADE AIRFOILS WITH PRESCRIBED

VELOCITY DISTRIBUTION

By Arthur W. Goldstein and Meyer Jerison

Flight Propulsion Research Laboratory
Cleveland, Ohio

Washington
May 1947

NATIONAL ADVISORY COMMITTEE FOR AERONAUTICS

TECHNICAL NOTE NO. 1308

ISOLATED AND CASCADE AIRFOILS WITH PRESCRIBED

VELOCITY DISTRIBUTION

By Arthur W. Goldstein and Meyer Jerison

SUMMARY

An exact solution of the problem of designing an airfoil with
a prescribed velocity distribution on the suction surface in a given
uniform flow of an incompressible perfect fluid is obtained by
replacing the boundary of the airfoil by vortices. By this device,
a method of solution is developed, which is applicable both to
isolated airfoils and to airfoils in cascade. The conformal
transformation of the designed airfoil into a circle can then be
obtained and the velocity distribution at any angle of attack
computed. Numerical illustrations of the method are given for the
airfoil in cascade.

INTRODUCTION

The problem of increasing the output per stage in axial-flow
compressors and turbines involves the use of high-solidity (closely
spaced blades) stages of highly cambered blades. In addition, the
velocity distribution must be carefully selected as a function of
arc length along the airfoil (blade section) boundary in order to
avoid flow separation or excessively high local velocities.

Several methods are available of obtaining an airfoil with a
prescribed velocity distribution when placed in a fixed position in
a uniform stream. The methods that lead to theoretically exact
results are based on conformal mapping theory. (See references 1
and 2.) In reference 3, Mutterperl extended the method of conformal
mapping to solve the problem of computing a cascade of airfoils with
prescribed velocity distribution but, for cascades with closely
spaced or highly cambered airfoils, this procedure becomes very
cumbersome. Approximate solutions have been obtained by placing
singularities such as vortices, sources, and sinks in a uniform
stream. Cascades of airfoils can also be computed by distributing

such singularities periodically throughout the region of the cas-
cade, as described by Ackeret (reference 4). Because these vor-
tex methods are not exact, a method has been developed with the
vortices on the boundaries of the cascade airfoils. This results
in a theoretically exact solution without the computation difficul-
ties encountered in conformal mapping methods for highly cambered
airfoils or closely spaced cascades. Furthermore, for the same
accuracy in computing the airfoil shape, this vortex method re-
quires the computation of fewer points than the method of conformal
mapping because these points may be arbitrarily placed on the airfoil.
The method may be applied to isolated airfoils and to airfoils in
cascade. For the cascade, the inflow and discharge velocities and
a velocity distribution on the surface of an airfoil are given and
the shape of the airfoil is determined. In some cases, the spacing
of the blades is preassigned, which places a condition on the as-
sumed velocity distribution. Before the airfoil shape has been
evolved, the velocity distribution may be computed for any angle
of attack by the method described in appendix A.

THEORY

Outline of Method

In reference 5, it is demonstrated that the two-dimensional
potential flow about a body in a uniform stream can be represented
by substituting for the body a sheet of vortices along its boundary.
The vortex strength per arc length at any point is equal to the
magnitude of the velocity at that point. A proof of this relation
for the case of the cascade is given in appendix B. The problem
of finding a shape with a prescribed velocity distribution when placed
in a stream can then be stated: given a vortex distribution, to find
a contour which satisfies the condition that it will be a streamline
in the flow field induced by the uniform flow and the vortices
distributed on the contour.

The procedure of finding the shape begins by choosing an
approximate shape and distributing the vortices on it. The stream
function of the flow induced by the vortices and the uniform stream
is computed at points on the boundary of the assumed shape. If
this stream function is constant, the assumed shape is correct.
Variations of the stream function are a measure of the deviation of
the assumed shape from the correct one. These variations are used
to distort the original shape into a new shape whose stream function
is more nearly constant. The process is repeated until the

variations become negligible. In the process of shape adjustment, the velocity is altered on the pressure surface.

Derivation of Equations for the Stream Function

Isolated airfoil. - The complex or reflected velocity $w'(z)$ (which is the derivative of the complex potential function $w(z)$) induced at the point z by a vortex of strength k located at z_o is

$$w'(z) = \frac{k}{2\pi i} \frac{1}{z - z_o}$$

A summary of the main symbols used in this report is given in appendix C.

The complex velocity, $w'(z)$ induced by a uniform stream with complex velocity w_u' and a distribution of vortex strength per unit length $\gamma(z_o)$ along a curve with coordinates z_o , is

$$w'(z) = w_u' + \frac{1}{2\pi i} \int \frac{\gamma(z_o) ds_o}{z - z_o} \tag{1}$$

where ds_o is the element of arc length along the curve. The complex potential at the point z is the integral of $w'(z)$ with respect to z , namely

$$w(z) = z w_u' + \frac{1}{2\pi i} \int \gamma(z_o) \log (z - z_o) ds_o \tag{2}$$

From reference 1 (notation modified)

$$\gamma(z_o) ds_o = w'(z_o) dz_o = dw(z_o) = d\varphi(z_o) + i d\psi(z_o)$$

where

φ velocity potential, $R[w(z)]$

ψ stream function, $I[w(z)]$

When equation (2) is applied to obtain the complex potential function at any point z in the flow field, the integration must be

carried out along the boundary of the body. Because this curve is a streamline, $d\psi = 0$ and, therefore, equation (2) becomes

$$w(z) = zw_u' + \frac{1}{2\pi i}\int \log (z-z_0) \, d\varphi(z_0) \qquad (2(a))$$

The imaginary part of equation (2(a)) is the stream function at the point z,

$$\psi = - xV_y + yV_x - \frac{1}{2\pi}\int \log \sqrt{(x-x_0)^2 + (y-y_0)^2} \, d\varphi(z_0) \qquad (3)$$

where

w_u' complex velocity of uniform stream for isolated airfoil, $(V_x - iV_y)$

z coordinate of point where stream function is computed, $(x + iy)$

z_0 coordinate of point where vortex is located, $(x_0 + iy_0)$

V_x x-component of uniform stream velocity V

V_y y-component of uniform stream velocity V

It is convenient to use the arc length along the airfoil as a parameter. If (x, y) is a point on the airfoil boundary, then s will denote the arc length there; similarly, s_0 will denote the arc length at (x_0, y_0). The vortex at s_0 on the airfoil influences the stream function at the point s on the airfoil. The stream function induced at (x, y) by a vortex of unit strength at (x_0, y_0) is

$$- f_1(z, z_0) = - \frac{1}{4\pi} \log \left[(x-x_0)^2 + (y-y_0)^2 \right] \qquad (4)$$

A plot in the (x, y) plane of curves for a constant $f_1(z, z_0)$ consists of concentric circles with center at (x_0, y_0).

The velocity at the point s_0 on the airfoil is the directional derivative $\varphi'(s_0)$ of the potential along the streamline. If the velocity along the airfoil has been specified and an airfoil shape has been assumed, the resultant stream function along the boundary

of the airfoil can be approximated by using the approximate shape in evaluating the integral

$$\psi(s) = \psi_u(s) - \int_0^l f_1(s, s_0) \varphi'(s_0) \, ds_0 \qquad (5)$$

where

$\psi_u(s)$ stream function at (x, y) due to uniform stream, $(-xV_y + yV_x)$

l total arc length of airfoil

All variables are expressed in terms of the arc-length parameters s and s_0. The integral in equation (5) can be evaluated either numerically or graphically over the entire range of integration except in the region where $a = s-s_0$ is small, for in this region $f_1(s, s_0)$ becomes infinite. This portion of the integral can be evaluated by approximating the airfoil boundary by a line segment. Then,

$$f_1(s, s_0) \approx \frac{1}{4\pi} \log (s-s_0)^2$$

The prescribed velocity can be given in this region, which may be defined by $s-a \leqq s_0 \leqq s+a$, by a Taylor expansion as a function of s_0 about the point s.

$$\varphi'(s_0) = \varphi'(s) + \varphi''(s)(s_0-s) + \frac{\varphi'''(s)}{2!}(s_0-s)^2 + \dots$$

where the primes indicate derivatives with respect to s. The integral is then

$$\int_{s-a}^{s+a} f_1(s, s_0) \varphi'(s_0) \, ds_0$$

$$= \int_{s-a}^{s+a} \frac{1}{4\pi} \log (s_0-s)^2 \left[\varphi'(s) + \varphi''(s)(s_0-s) + \dots \right] ds_0$$

$$= \frac{1}{\pi} \left[a \varphi'(s)(\log a-1) + \frac{a^3 \varphi'''(s)}{3!}\left(\log a - \frac{1}{3}\right) + \dots \right] \qquad (6)$$

In most cases it is necessary to use only the first term in equation (6). The same type of approximation can be used to evaluate a portion of the integral if the opposite side of the airfoil comes in the neighborhood of the point (x, y).

A more general equation applicable to a segment that does not pass through s is:

$$\frac{1}{4\pi}\int_{p+b}^{p+c} \log\left[(x-x_0)^2 + (y-y_0)^2\right] \varphi'(s_0)\, d(s_0)$$

$$= \frac{1}{4\pi}\left\{\varphi'(p)\left[c \log(h^2+c^2) - b \log(h^2+b^2) - 2(c-b) + 2h \tan^{-1}\frac{h(c-b)}{h^2+bc}\right]\right.$$

$$+ \frac{\varphi''(p)}{2!}\left[(h^2+c^2)\log(h^2+c^2) - (h^2+b^2)\log(h^2+b^2) - (c^2-b^2)\right]$$

$$+ \frac{\varphi'''(p)}{3!}\left[c^3 \log(h^2+c^2) - b^3 \log(h^2+b^2) - \frac{2}{3}(c^3-b^3)\right.$$

$$\left.\left. + 2h^2(c-b) - 2h^3 \tan^{-1}\frac{h(c-b)}{h^2+bc}\right] + \ldots\right\} \qquad (6(a))$$

where h is the perpendicular distance from s to the segment, $s_0 = p$ locates the foot of the segment, $(p+b)$ and $(p+c)$ are the limits of the integration of s_0, and approximately,

$$\varphi'(p) = \varphi'(p+b) - b\,\varphi''(p+b) + \frac{b^2}{2}\,\varphi'''(p+b)$$

$$\varphi''(p) = \varphi''(p+b) - b\,\varphi'''(p+b)$$

$$\varphi'''(p) = \varphi'''(p+b)$$

Equation (6(a)) may be used when the line segment is not of equal lengths on either side of the perpendicular foot or when $\varphi'(s)$ or its derivatives are discontinuous at either $(p+b)$ or $(p+c)$. If $a = c = -b$ and $h = 0$, equation (6(a)) reduces to equation (6).

The size of a, b, or c is determined by the requirements that the segment in question be nearly straight (the approximation is of the second degree) and that $\varphi'(s_0)$ be accurately represented by a Taylor series expansion of few terms.

Airfoils in cascade. - The expression for the complex potential for the flow about a cascade of airfoils is derived in appendix B. The notation is defined in figure 1. The formula, which corresponds to equation (2(a)) for isolated airfoils, is

$$w(z) = zw_m' + \frac{1}{2\pi i} \int \log \left[\sin \left(\frac{\pi}{d}\right) (z-z_0) \right] d\varphi(z_0) \tag{7}$$

where

d   distance between successive airfoils in cascade

w_m' mean stream velocity, which is one half the sum of complex (reflected) velocities upstream and downstream of cascade, $V_x - iV_y$

The mean velocity w_m' corresponds to the uniform velocity w_u' of the isolated airfoil flow.

The term zw_m' is the complex potential function resulting from the mean flow. In the integral, the element $d\varphi$ indicates the vortex element strength and $-\log [\sin (\pi/d) (z-z_0)]$ represents the complex potential at the point z caused by an infinite row of unit vortices at $z_0 \pm nd$ where n = 0, 1, 2, ... The imaginary part of equation (7) is the stream function,

$$\psi(s) = \psi_m(s) - \int_{s_0=0}^{s_0=\ell} f_2(s, s_0) \, d\varphi(s_0) \tag{8}$$

where

$$f_2(s, s_0) = \frac{1}{4\pi} \log \left[\sin^2 \frac{\pi}{d} (x-x_0) + \sinh^2 \frac{\pi}{d} (y-y_0) \right]$$

is expressed in arc-length parameters and $\psi_m(s)$ is the stream function at (x, y) induced by a mean stream whose complex velocity is w_m'; that is,

$$\psi_m = - xV_y + yV_x$$

The values of $\frac{(x-x_0)}{d}$ and $\frac{(y-y_0)}{d}$ for various values of f_2 are given in table I. A plot of $x-x_0$ and $y-y_0$ for constant values of $f_2(z, z_0)$ is shown in figure 2. These curves may be interpreted as the streamlines of the flow induced by an infinite row of vortices of unit strength located at the points $(x_0 \pm nd, y_0)$, where $n = 0, 1, 2, \ldots$. In the region of a vortex, the streamlines are nearly circles; that is, the flow is nearly that induced by an isolated vortex. At a distance from the vortex row, the streamlines are parallel lines, as in the flow pattern induced by a continuous uniform distribution of vorticity along a straight line instead of a row of discrete vortices. The velocities on the two sides of such a vortex line are of equal magnitude but opposite direction.

This behavior of f_2 for large $\frac{|y-y_0|}{d}$ and also for small $\frac{[(y-y_0)^2 + (x-x_0)^2]}{d^2}$ can be described as follows: When both $\frac{x-x_0}{d}$ and $\frac{y-y_0}{d}$ are small,

$$f_2(z, z_0) \approx \frac{1}{4\pi} \log \frac{\pi^2}{d^2} \left[(x-x_0)^2 + (y-y_0)^2 \right] \tag{9}$$

which differs from $f_1(z, z_0)$ only by a constant. For large values of $\frac{|y-y_0|}{d}$, irrespective of $\frac{x-x_0}{d}$ and a constant term,

$$f_2(z, z_0) \approx \frac{|y-y_0|}{2d} \tag{10}$$

which is the stream function of a uniform stream parallel to the x-axis.

Equation (8) can be used for computing the stream function along the boundary of an airfoil in cascade just as equation (5) is used for the isolated airfoil. The integral over the range in the neighborhood of the point s is obtained by using equation (9) for $f_2(s, s_0)$. The result, derived in the same manner as equation (6), is

$$\pi \int_{s-a}^{s+a} f_2(s, s_0)\, \varphi'(s_0)\, ds_0$$

$$= \left\{ a\, \varphi'(s) \left[\log\left(\frac{\pi}{d}\, a\right) - 1 \right] + a^3\, \frac{\varphi'''(s)}{3!} \left[\log\left(\frac{\pi}{d}\, a\right) - \frac{1}{3} + \ldots \right] \right\}$$

$$(6(b))$$

The more general equation (6(a)) is modified for cascades by multiplying the argument of all logarithms by the factor π^2/d^2.

Adjustment of Shape

If the stream function for the assumed airfoil has been computed and has been found to vary, the shape must then be adjusted to give a more nearly constant stream function. The shape changes are made by rotation of the body, plus displacement of the individual points normal to the mean stream. A succession of such changes results in the most general type of shape distortion. The rotation is used to place the front stagnation point properly.

Rotation of the airfoil. - In the formula for computing the stream function of an isolated airfoil, the contribution of a vortex element at (x_0, y_0) to the stream function of a point at (x, y) is dependent merely on the distance between the two points. Consequently, if the entire airfoil is rotated, the effect of the boundary vortices on the stream function at any point on the airfoil boundary will not change. The effect of the blade rotation on the stream function along the boundary is therefore determined by the change in relative position of the points in the uniform stream. The first adjustment in shape is a rigid rotation of the airfoil in order to obtain a more nearly constant stream function along its boundary.

If the airfoil is rotated through an angle β, the stream function is so changed that $\psi(s)$ is a function of β and s and may be written $\psi(s, \beta)$. When $\beta = 0$, $\psi(s, 0)$ is the original stream function before rotation. After rotation the new stream function $\psi(s, \beta)$ may be expanded in a Taylor series about the point $\beta = 0$,

$$\psi(s, \beta) = \psi(s, 0) + \beta \left[\frac{\partial \psi(s, \beta)}{\partial \beta} \right]_{\beta=0} + \ldots$$

Only the first two terms in this series will be used because it is
assumed that β is small. The angle β is to be determined for
the minimum mean-square deviation of the stream function from its
mean value. Because the object of the rotation is essentially to
adjust the shape of the nose, the rotation might also be made to
reduce the root-mean-square deviation of the stream function to a
minimum for a portion of the shape including the nose.

The mean value of the stream function at any angle β is

$$\bar{\psi}(\beta) = \frac{1}{l}\int_0^l \psi(s,\ \beta)\ ds = \frac{1}{l}\int_0^l \left[\psi(s,\ 0) + \beta\left(\frac{\partial\psi}{\partial\beta}(s,\ \beta)\right)_{\beta=0}\right] ds \quad (11)$$

The difference between the new stream function $\psi(s,\ \beta)$ and its mean
value $\bar{\psi}(\beta)$ is squared and integrated to obtain a measure of the
variation of $\bar{\psi}(s,\ \beta)$ from the mean value at the new angle. The
condition for obtaining a minimum root-mean-square deviation by
adjusting β is

$$0 = \frac{d}{d\beta}\int_0^l \left[\psi(s,\ \beta) - \bar{\psi}(\beta)\right]^2 ds = \frac{d}{d\beta}\int_0^l \left[\bar{\psi}(s,\ 0) + \beta\ \frac{d\psi(s,\ 0)}{d\beta} - \bar{\psi}(\beta)\right]^2 ds$$

$$= \int_0^l 2\left[\psi(s,\ 0) + \beta\ \frac{d\psi(s,\ 0)}{d\beta} - \bar{\psi}(\beta)\right]\left[\frac{d\psi(s,\ 0)}{d\beta} - \frac{d\bar{\psi}(\beta)}{d\beta}\right] ds \quad (12)$$

$$2\int_0^l \frac{d\psi(s,\ 0)}{d\beta}\left[\psi(s,\ 0) + \beta\ \frac{d\psi(s,\ 0)}{d\beta} - \bar{\psi}(\beta)\right] ds$$

$$- 2\ \frac{d\bar{\psi}(\beta)}{d\beta}\int_0^l \left[\psi(s,\ 0) + \beta\ \frac{d\psi(s,\ 0)}{d\beta} - \bar{\psi}(\beta)\right] ds = 0 \quad (13)$$

The second integral vanishes by virtue of equation (11), which may
also be used to eliminate $\bar{\psi}(\beta)$ from the remaining term. The solution
for β is

$$\beta = \frac{\int_0^l \psi(s)\ \frac{d\psi(s,\ 0)}{d\beta}\ ds - \frac{1}{l}\left[\int_0^l \psi(s)\ ds\right]\left[\int_0^l \frac{d\psi(s,\ 0)}{d\beta}\ ds\right]}{\frac{1}{l}\left[\int_0^l \frac{d\psi(s,\ 0)}{d\beta}\ ds\right]^2 - \int_0^l \left[\frac{d\psi(s,\ 0)}{d\beta}\right]^2 ds} \quad (14)$$

In order to apply equation (14), $d\psi/d\beta$ must be known at points along the boundary of the airfoil. In the case of the isolated airfoil, the contribution of the vortices is unaffected by the rotation and therefore,

$$\frac{d\psi}{d\beta} = \frac{d\psi_u}{d\beta} = \frac{d}{d\beta} \left(-xV_y + yV_x \right) = -V_y \frac{dx}{d\beta} + V_x \frac{dy}{d\beta} \tag{15}$$

If the airfoil is rotated about the point (x_c, y_c), equation (15) becomes

$$\frac{d\psi}{d\beta} = \cos\beta \left[(x-x_c) V_x + (y-y_c) V_y \right]$$

$$+ \sin\beta \left[(x-x_c) V_y - (y-y_c) V_x \right] \tag{16}$$

where (x, y) are the coordinates of the point before rotation. For small values of β, equation (16) reduces to

$$\frac{d\psi}{d\beta} = (x-x_c) V_x + (y-y_c) V_y \tag{17}$$

The choice of (x_c, y_c) will have no effect on the results in this case.

When the airfoil in cascade is rotated, the change in the position of the vortices of the adjacent blade must be considered. In the case of the isolated airfoil, it was unnecessary to consider the change in position of the vortices because the influence of a vortex (equations (3), (4), and (5)) depended on the function f_1, which is constant on circles. The influence of the vortices on the airfoil is therefore independent of direction. Because the f_2 contours are not circles, the rotation in cascade does have an effect, which is approximated by considering all closed f_2 curves ($f_2 < 0$) as circles in order that the effect of all vortices in the region $f_2 < 0$ may be neglected during rotation. The effect of all vortices in the region $f_2 > 0$ is estimated by assuming that all the f_2 contours for $f_2 > 0$ are straight lines uniformly spaced. The flow corresponds to that between two infinite straight parallel vortex sheets of uniform strength per unit length. This flow induced by the vortices in the region $f_2 > 0$ is in the

x-direction, and the direction of the flow induced by the vortices
for which $y_o > y$ is opposite in sense to that induced by the vortices
for which $y_o < y$.

As the point being considered is changed, the regions for
$f_2 > 0$, $y_o > y$, and $f_2 > 0$, $y_o < y$ will include different sections
of the blades, and hence different vorticity, with the result that
the x-velocity component v_x induced by the vortex sheets will vary
with the point under consideration. The algebraic sum of the
x-component of the uniform flow velocity and the variable x-velocity v_x
induced by the vortices in the region $f_2 > 0$ is to be used like the
velocity component V_x in rotation of the isolated airfoil (equa-
tion (17)). The quantity V_x in equation (17) is replaced by the corre-
sponding $V_{x,r}$ ($= V_x + v_x$). The vortex strength per unit length at any
point on the airfoil is equal to $\varphi'(s_o)$ and, therefore, from equa-
tion (10) the x-component of the velocity induced by the vortices is

$$\frac{1}{2d}\int \varphi'(s_o)\, ds_o,$$ where the integration is carried out over the portion

of the airfoil where $f_2(s, s_o) > 0$. A distinction must be made between
the two regions $y_o < y$ and $y_o > y$ because the induced components have
opposite direction.

The computed result of rotating an airfoil in cascade depends upon
the choice of (x_c, y_c) because $d\psi/d\beta$ is only approximate. In order
to minimize the error involved, values of $d\psi/d\beta$ are reduced by
choosing (x_c, y_c) as the centroid of the vortex distribution on the
airfoil. If the improvement in the mean-square deviation of ψ is
small compared with its original value, it may be preferable to omit
the rotation of the airfoil because of the error inherent in the computa-
tion. The decision should be made chiefly on how ψ varies at the air-
foil nose and whether it is approaching a constant value in this region
with successive corrections of the shape.

Distortion of the shape. - The stream function computed after the
isolated airfoil has been rotated will, in general, still vary along
the boundary. This variation can be reduced by distorting the shape of
the airfoil. If the distortion is small, the change in distance between
any two points on the boundary will be small, although the change in the
direction of a segment joining those points may be considerable. The
effect of the distortion on the contribution to the stream function of
the vortices on the boundary is consequently neglected. The largest
effect of the distortion will be to change the position of the boundary
points in the uniform stream. The airfoil is therefore distorted in such
a manner that the change in the contribution of the uniform stream to the

stream function will eliminate the variations in stream function. For points directly opposite each other on the airfoil, the change in distance will be of the same order of magnitude as the distortion. Consequently, distortions that result in change of thickness of the airfoil converge very slowly because of the inaccuracy of the fundamental assumption on which the correction is based.

Thus, when the stream function along the boundary of the isolated airfoil is known, some number is arbitrarily chosen as the desired constant value of the stream function. If $\Delta\psi = \psi - \overline{\psi}$ is the difference between the computed stream function at a point and the desired constant, the point is moved a distance $-\Delta\psi/V$ perpendicular to the direction of the mean stream, where the direction of increasing uniform stream function is taken as positive. The airfoil in a cascade is distorted in the same manner, using the varying resultant local mean stream velocity $\sqrt{V_{x,r}^2 + V_y^2}$; corrections are made with $\overline{\psi}$ equal to the mean value of ψ on the airfoil.

COMPUTATIONAL PROCEDURE FOR CASCADES

Choice of Velocity Distribution

Several factors influence the choice of the velocity distribution for which an airfoil is to be found. Especially in rotors, sturdy blades are required. Long thin tail sections must be avoided and where high rotative speeds and stresses occur, overhang of thin sections is likely to induce blade failure. The radial distribution of airfoil cross-sectional area is also fundamental in determining the blade-root stresses. Overhang can be reduced by proper choice of the velocity diagrams for the sections, but the other factors are influenced chiefly by the thickness of the section.

The desired thickness may be attained by first assuming a blade shape and spacing and using the stream-filament method of reference 6 to compute the velocity distribution over a portion of the airfoil that determines the thickness. The spacing may be regarded as fixed but the curvature can be adjusted if local velocities are too high for the desired thickness. This computed velocity will then serve as a guide to the choice of an airfoil velocity distribution, which should be chosen to avoid high velocity peaks and steep negative gradients. If the average of the velocities on opposite sides of the blade camber line is retained in the modification of the velocity distribution computed from the stream-filament method, the thickness will also be retained.

Because of the irrotationality of the fluid motion, the velocity integral or circulation around the airfoil must be equal to that around a blade but over a width equal to one blade space. Therefore,

$$\int \varphi'(s)\ ds = \Gamma = d(V_{x,1} - V_{x,2})$$

where

$V_{x,1}$ tangential velocity entering cascade

$V_{x,2}$ tangential velocity leaving cascade

Γ circulation about airfoil

This relation places a condition on the assumed velocity distribution.

If the computations thus far have been made in order to select a velocity distribution for the airfoil cascade in a compressible fluid flow, an equivalent velocity distribution for the flow of an incompressible fluid must be determined before the blade shape can be computed by any method based on incompressible flow theory. For subcritical flows the directions of the incoming and discharge velocities are the same for compressible and incompressible flows, but for incompressible flow the component normal to cascade axis is the same upstream and downstream. The Kármán-Tsien compressibility correction (reference 7) or that of Garrick and Kaplan (reference 8) may be applied to the velocity on the blade surface to estimate roughly the corresponding incompressible flow velocity distribution. The resulting velocity distribution in any case must satisfy the circulation condition. This procedure does not give an exact solution for compressible flows, but the resultant compressible flow will have approximately the desired characteristics of low pressure gradients and no high velocity peaks.

Computation of Airfoil Shape from the

Chosen Velocity Distribution

The numerical computation of the quantities involved in the preceding analysis, particularly the function f_2, is extremely laborious when tables of $f_2(s, s_0)$ are used. Most of the computations are therefore executed graphically. In the cascade example, it was assumed that the air entered the cascade at an angle of 45° from the

cascade axis and was discharged at an angle of -30° from the cascade
axis. The assumed velocity distribution is given in figure 3(a).
The value of the lift coefficient for this airfoil is 3.1. The
shapes of the isolated airfoil and the airfoil in cascade are
computed by the following steps:

1. Curves for constant f_1 for the isolated airfoil, or
constant f_2 (fig. 1) for the airfoil in cascade, are drawn. This
diagram should be made on some transparent material that will neither
change size nor shape. The coordinates of the curves for constant f_2
are given in table I.

2. A desired velocity $\varphi'(s)$ is chosen as a function of the
arc length of the airfoil (fig. 3(a)). An airfoil shape having the
desired total arc length is assumed and is drawn to the same scale
as the plot of f_1 or f_2. The drawing is made on grid paper and,
in the case of a cascade, the x-axis is taken along the cascade
axis (fig. 4).

3. The velocity distribution $\varphi'(s)$ is integrated to obtain
the velocity potential $\varphi(s)$. This function is plotted on the same
chart as the assumed airfoil shape for the corresponding y-coordinate,
as shown in figure 4, by plotting both φ and the y-coordinate of
the airfoil against s on a supplementary graph. In regions of the
airfoil where y varies little with s, that is, where the airfoil
boundary is parallel to the x-direction, φ should be plotted
against x in the same manner, as shown in figure 4.

4. In order to find the stream function at a point (x, y)
on the airfoil, a plot of $f_2(s, s_0)$ as a function of $\varphi(s_0)$ must
be obtained to evaluate the quantity $\int f_2(s, s_0) \, d\varphi(s_0)$ of equa-
tion (8). If the chart of f_2 is superimposed on the airfoil with
one vortex center overlaying the point (x, y), the value of f_2
may be read at (x_0, y_0) and the corresponding value of $\varphi(x_0, y_0)$
may also be read from the plot of $\varphi(x_0, y_0)$. The value of $f_2(s, s_0)$
is the same as would have been obtained by centering the chart on
(x_0, y_0) because of the symmetry of the function. A succession of
values of φ and f_2 are obtained in this fashion for various posi-
tions (x_0, y_0) that intersect the f_2 contours, and a plot of
these points (f_2, φ) may be made for the assumed position (x, y).
This procedure is illustrated in figure 5 for a particular point
(x, y) on which the f_2 chart is centered. The readings for a
particular (x_0, y_0) are shown by the arrowed lines. The

points 1 to 6 on the blade are shown on the corresponding f_2 curve.
The discontinuity of φ between points 1 and 6 is the circulation.
The discontinuity between 4 and 5 represents the region where f_2
approaches $-\infty$.

5. The proper method of integration then proceeds from 1 through
6 to 7 and then to the origin, with constant f_2 from 4 to 5. The
region from 4 to 5 with f_2 approaching $-\infty$ is computed by equa-
tion (6) or (6(b)); the constant a is assumed to be the radius of
the near-circle, which corresponds to the value of f_2 where the
discontinuity from 4 to 5 occurs.

The total area including this small addition is

$$\int \varphi'(s_0) \, f_2(s, \, s_0) \, ds = \int f_2(s, \, s_0) \, d\varphi$$

which is the stream function due to vortices on the entire set of
airfoils in cascade. Where $f_2 = 0$ at the points A, B, C, and D
(fig. 5), the values of φ are noted as $\varphi_A(s)$, $\varphi_B(s)$, $\varphi_C(s)$,
and $\varphi_D(s)$. These values are used in computing the stream-function
change caused by rotating the blade. The stream function at the
point $(x, \, y)$ may now be computed from equation (8) or (5), and

$$\psi_m = -V_y x + V_x y$$

A plot of the stream function (variation from the mean value)
is shown in figure 6 for the initially assumed shape. Corresponding
points on adjacent airfoils have a difference of $\Delta\psi/V_y d$ equal to 1.0.

6. When $\psi(s)$ is known at a sufficient number of points, the
airfoil may be rotated as previously described. For the isolated air-
foil, equations (14) and (17) may be used directly. For the airfoil
in cascade, the coordinates of the centroid of the airfoil must first
be computed by

$$x_c = \frac{1}{\Gamma} \oint x \, \varphi'(s_0) \, ds_0$$

$$y_c = \frac{1}{\Gamma} \oint y \, \varphi'(s_0) \, ds_0$$

Before equation (17) can be used to compute $d\psi/d\beta$, the variable quantity $V_{x,r}$ must be computed. The vortices in the region $f_2 > 0$ are considered to be uniformly distributed along the cascade axis and the velocity induced by such a distribution is

$$v_x = \pm \frac{\gamma}{2}$$

where γ is the vortex strength per unit length along the cascade axis for $f_2 > 0$. Therefore,

$$v_x = \frac{1}{2d} \int \varphi'(s_0)\ ds_0$$

where the integral is to be taken over the regions $f_2 > 0$. The region $f_2 > 0$, $y_0 > y$ contributes a positive component to v_x, whereas the region $f_2 > 0$, $y_0 < y$ contributes a negative component. The computation is simply carried out by making use of the fact that the integral for v_x is the difference between values of φ at points where $f_2 = 0$. The values of $\varphi_A(s_0)$, $\varphi_B(s_0)$, $\varphi_C(s_0)$, and $\varphi_D(s_0)$ from step (5) are used at this point to obtain

$$2v_x d = \int \varphi'(s_0)\ ds_0 = \varphi_A - \varphi_D + \Gamma - (\varphi_C - \varphi_B) \tag{18}$$

where Γ is introduced because of the discontinuity in φ at the trailing edge. The term $\varphi_A - \varphi_D + \Gamma$ gives the effect of the vorticity in the region $f_2(s, s_0) > 0$ near the trailing edge, and the term $\varphi_C - \varphi_B$ gives the effect of the vorticity in the region $f_2(s, s_0) > 0$ near the leading edge. If either the leading edge or the trailing edge lies in the region $f_2(s, s_0) < 0$, only two points of intersection will remain and one of the two groups of terms in equation (18) will vanish. The quantity $\frac{1}{2d} \int \varphi'(s_0)\ ds_0$ is added to the x-component of the original uniform stream velocity and the quantity $d\psi/d\beta$ of equation (17) may be computed for a number of points and the angle β computed from equation (14), using the values of (x_c, y_c) just determined. After these computations have been made, the airfoil is rotated through the angle β, and the value $\psi + \beta \frac{d\psi}{d\beta}$ is assigned as the value of the stream function of the point after rotation.

7. A value of $\psi(s)$ is known at points along the airfoil boundary. The mean value over the airfoil $\bar{\psi}$ is subtracted from ψ leaving $\Delta\psi$. For the isolated airfoil, no subtraction is necessary. Each point is

moved a distance $-\dfrac{\Delta\psi}{\sqrt{V_{x,r}^2 + V_y^2}}$ in the direction perpendicular to

the velocity computed in step 6. The curve joining the points in their new positions is the adjusted airfoil.

8. The total arc length of the adjusted airfoil will be different from the original one, in general, although local changes in length will be negligible. The airfoil is so scaled that the length of the suction side is the same length as it had been before distortion because this surface is the critical surface of the airfoil. This process will result in a change in length of the pressure side. The velocity over the pressure side $\varphi'(s)$ must then be altered in such a manner that the difference in potential between the two stagnation points remains the same. As a result, the quantities that retain specified values are the length and the velocity distribution on the suction side and the circulation around the airfoil. The entire procedure is repeated with the adjusted shape until the variations in the stream function result in very little change in the shape of the airfoil.

Discussion of Examples and Techniques

For the example being computed, the stream functions obtained for the initially assumed shape and the first and seventh approximations are plotted against the arc length (fig. 6), which is taken as zero at the trailing edge and proceeds counterclockwise around the airfoil as shown in figure 7. The fact that $\Delta\psi$ for the initial shape is positive over the first half of the arc length and negative over the second half indicates that it is too thick because the required distortion in shape will make it thinner. The change in thickness results in a change in velocity distribution over the pressure side of the airfoil in order to maintain the desired circulation. The velocity that was originally assumed, which is equal to the vorticity per unit length distributed on the initial airfoil, is shown in figure 3(a) and the velocity over the final shape in figure 3(b). The length of the pressure side has increased and the velocity has decreased in the proportion of 1:1.1.

Over the section of the airfoil that has collapsed to zero thickness, the surface velocities of figure 3(b) may not have been obtained, but the loading (circulation per unit arc length), which is the

difference in the velocities on opposite sides, has been realized. In practice, this collapse is prevented by increasing the assumed velocity on the airfoil surface.

If the initially assumed airfoil shape has a thickness that differs considerably from the correct one, the process of shape adjustment will converge rather slowly. The labor can be reduced, however, by computing the stream function at a few points on the airfoil and locating these points to determine the thickness. This procedure is followed for the first few approximations until the thickness of the airfoil is fairly accurate. The stream function is then computed at a larger number of points, particularly near the leading edge, in order to get more detail of the shape.

If a velocity distribution is arbitrarily specified, the resulting shape may not be a physically real airfoil but may result in a figure-8 or a collapsed shape (zero thickness over a portion of the blade). It is then necessary to modify the velocity distribution to obtain a real shape; these modifications should be selected to keep the desirable properties of the original distribution. Velocity peaks and steep velocity gradients, which tend to occur on the suction side of an airfoil, are to be avoided. If the airfoil collapses, the vorticities of the two sides tend to cancel each other and the remaining vorticity represents the difference in velocity across the thin airfoil rather than the velocity along the boundary.

The method was also applied to the design of a thin airfoil (camber line) in a cascade. The vortex distribution is equivalent to load distribution (difference in velocity across the airfoil) rather than velocity as in the case of a thick airfoil. The velocity diagram for the cascade and the desired velocity difference are shown in figure 8. The value of the lift coefficient of the resultant airfoil is 4.1. The initial shape was obtained by assuming zero spacing between the airfoils. The initial shape and the first and third approximations to the airfoil shape are shown in figure 9. There is very little difference between the second and third approximations. The third approximation is redrawn in this diagram to show the spacing between airfoils. The convergence of the method is shown graphically in figure 10. The variation $\Delta\psi$ of the stream function from its mean is divided by Vd to make it dimensionless and is plotted against the arc length along the airfoil where $s = 0$ at the trailing edge. The stream function

computed on the second approximation is nearly constant, which gives
the third approximation almost the same shape as the second one.
The rapid adjustment of camber contrasts with the slow adjustment
of thickness.

Flight Propulsion Research Laboratory,
    National Advisory Committee for Aeronautics,
        Cleveland, Ohio, March 4, 1947.

APPENDIX A

VELOCITY DISTRIBUTION ON THE DERIVED AIRFOIL

AT DIFFERENT FLOW ANGLES

Conformal mapping. - When an airfoil is given, the velocity distribution over its surface must frequently be found at different angles of attack. This problem may be solved by the method of conformal mapping, which consists of mapping the region exterior to the airfoil on the exterior of a circle. The velocity around the airfoil is obtained from the known velocity around the circle. Procedures for finding the function that maps a given airfoil into a circle are presented in references 1 and 9 for the isolated airfoil and references 3 and 10 for the airfoil in cascade.

In general, the procedure for finding the mapping function of an airfoil is a laborious one. But when, as in the present case, the velocity distribution over the airfoil at a particular angle of attack is known, the correspondence between points on the airfoil and on the circle, and hence the flow velocity at other angles of attack, can be obtained very easily. Indeed, the correspondence of points and the velocities for various angles of attack can be obtained by the method of Weinig and Gebelein (reference 11) from the initial data without knowing the airfoil shape, because the complex potentials of the airfoil plane and the mapping circle plane are equal. Before the airfoil is designed, therefore, it is possible to check whether the airfoil to be computed will be satisfactory under conditions different from the design condition.

Isolated airfoil. - The flow about any airfoil shape can be mapped on the flow about a unit circle in such a way that corresponding points have the same potential. The flow about the airfoil is given and the potential function $\varphi(s)$ at each point is computed. If the potential function on the airfoil is computed by integrating the velocity from the stagnation point at the trailing edge in a counterclockwise direction around the airfoil oriented like the one in figure 1, the potential will be zero at the trailing edge, decrease to a minimum φ_{min} at the stagnation point at the leading edge, and then increase to a value equal to the circulation Γ at the trailing edge. The corresponding flow about the circle is determined by the conditions that it must have the same values of φ_{min} and Γ for a correspondence to

exist between all airfoil and circle points. If θ_T is the central angle of the stagnation point on the circle that corresponds to the trailing edge of the airfoil,

$$\frac{\pi \varphi_{min}}{\Gamma} = -(\cot \theta_T + \theta_T + \pi/2) \tag{A1}$$

Equation (A1) can be solved numerically for θ_T because all the other quantities are known. The velocity at infinity in the circle plane V_c can then be determined from the Kutta-Joukowsky condition, which requires that θ_T be a stagnation point; that is,

$$V_c = -\frac{\Gamma}{4\pi \sin \theta_T} \tag{A2}$$

The velocity potential at points on the circle is

$$\varphi_c = -2V_c \cos \theta + \frac{\Gamma \theta}{2\pi} + 2V_c \cos \theta_T - \frac{\Gamma}{2\pi} \theta_T \tag{A3}$$

The quantity $2V_c \cos \theta_T - \frac{\Gamma}{2\pi} \theta_T$ is a constant that is subtracted in order to make $\varphi_c = 0$ at the stagnation point corresponding to the trailing edge.

The correspondence of points on the airfoil with points on the circle is obtained by associating points where $\varphi(s) = \varphi_c$. The velocity on the circle at a uniform stream flow angle α_1 is

$$v_c(\theta,\alpha_1) = 2V_c \left[\sin(\theta + \alpha_1) - \sin(\theta_T + \alpha_1) \right] \tag{A4}$$

The nature of the conformal transformation is such that the ratio of the velocity at a point on the airfoil to the velocity at the corresponding point on the circle is independent of angle of attack. Therefore, the velocity $\varphi_1'(s)$ on the airfoil at flow angle α_1 is

$$\frac{\varphi_1'(s)}{v_c(\theta,\alpha_1)} = \frac{\varphi'(s)}{v_c(\theta,0)} \tag{A5}$$

where the design flow angle is taken as zero. Equation (A5) can be used to compute the velocity distribution on the airfoil except at the two points that were stagnation points at the design angle of attack.

Airfoils in cascade. - The flow about a cascade of airfoils can be mapped conformally into the flow about a unit circle with two singular points located on the real axis symmetrically with respect to the center of the circle. These singular points correspond to the points at infinity in front of and behind the cascade, respectively. In a cascade of airfoils, the distance of these points from the center of the circle is uniquely determined by the same conditions that determine the flow about the circle in the isolated case; namely, the circulation per airfoil, the velocity potential at the leading edge, the blade spacing, and the upstream and downstream flow angles.

The distance from the singular points to the center of the circle is denoted by e^K. The flow about the circle is such that the location of the stagnation points θ_T is determined by the relation

$$- \frac{\Gamma}{2Vd} = \frac{\sin \theta_T}{\sinh K} \cos \lambda + \frac{\cos \theta_T}{\cosh K} \sin \lambda \qquad (A6)$$

where λ is the angle of inclination of the mean stream to the normal to the cascade axis. (See reference 6 for details). The quantities Γ, V, d, and λ are known from the flow in the cascade plane and therefore equation (A6) provides a relation between K and the location of the stagnation points.

The velocity potential at any point on the circle is

$$\varphi_{c,c} = \frac{Vd}{\pi} \left(\sin \lambda \tan^{-1} \frac{\sin \theta}{\sinh K} - \cos \lambda \tanh^{-1} \frac{\cos \theta}{\cosh K} \right)$$

$$+ \frac{\Gamma}{2\pi} \tan^{-1} \frac{\tan \theta}{\tanh K} - \left[\frac{Vd}{\pi} \left(\sin \lambda \tan^{-1} \frac{\sin \theta_T}{\sinh K} - \cos \lambda \tanh^{-1} \frac{\cos \theta_T}{\cosh K} \right) \right.$$

$$\left. + \frac{\Gamma}{2\pi} \tan^{-1} \frac{\tan \theta_T}{\tanh K} \right] \qquad (A7)$$

The expression in brackets is a constant so chosen that the potential will vanish at the stagnation point corresponding to the trailing edge of the airfoil. In order to map the cascade on the circle, it is required to find K so that the value of $\varphi_{c,c}$ at θ_N, the stagnation point corresponding to the leading edge of the airfoil, is equal to φ_{min}, the value of the velocity potential there. In successive approximations, a value of K is assumed and equation (A6) is solved simultaneously with the identity

$$\left(\frac{\sin \theta}{\sinh K}\right)^2 \sinh^2 K + \left(\frac{\cos \theta}{\cosh K}\right)^2 \cosh^2 K \equiv 1$$

for the variables $\dfrac{\sin \theta}{\sinh K}$ and $\dfrac{\cos \theta}{\cosh K}$. The solutions of these equations are

$$\frac{\sin \theta_s}{\sinh K} = \frac{-\dfrac{\Gamma}{2Vd} \cosh^2 K \sin \lambda \pm \cos \lambda \sqrt{\cosh^2 K - \cos^2 \lambda - \left(\dfrac{\Gamma}{2Vd}\right)^2 \cosh^2 K \sinh^2 K}}{\cosh^2 K - \cos^2 \lambda}$$

and $\dfrac{\cos \theta_s}{\cosh K}$ obtained from equation (A6). These solutions, $\left(\dfrac{\sin \theta_N}{\sinh K}, \dfrac{\cos \theta_N}{\cosh K}\right)$ and $\left(\dfrac{\sin \theta_T}{\sinh K}, \dfrac{\cos \theta_T}{\cosh K}\right)$, are substituted in equation (A7) to find the value of $\varphi_{c,c}$ at $\theta = \theta_N$. If $\varphi_{c,c}(\theta_N)$ is not equal to φ_{min}, another value of K is chosen, on the premise that $\varphi_{c,c}(\theta_N)$ will decrease as K is decreased. When $\varphi_{c,c}(\theta_N)$ is evaluated, care should be taken to use consistent values of the inverse tangents. After two values of K and $\varphi_{c,c}(\theta_N)$ are determined, interpolation or extrapolation may be used for new values of K.

When K has been found, it is used in equation (A7) to evaluate $\varphi_{c,c}$ at values of θ all around the circle. A point on the circle corresponds to the point on the airfoil where $\varphi(s) = \varphi_{c,c}$. The velocity at the point θ on the circle is

$$v_{c,c}(\theta,\alpha) = \frac{Vd}{\pi} \frac{\sinh 2K}{\cosh 2K - \cos 2\theta}\left[\cos \lambda \left(\frac{\cos \theta}{\cosh K} - \frac{\cos \theta_T}{\cosh K}\right)\right.$$

$$\left. + \sin \lambda \left(\frac{\sin \theta}{\sinh K} - \frac{\sin \theta_T}{\sinh K}\right)\right] \tag{A8}$$

and the velocity on the airfoil at any other mean flow angle λ_1 is

$$\varphi_1{}'(s) = v_{c,c}(\theta,\lambda_1) \; \frac{\varphi'(s)}{v_{c,c}(\theta,\lambda)} \tag{A-9}$$

as in the case of the isolated airfoil.

The designed airfoil was mapped on the unit circle by the method described. The constant K, the natural logarithm of the distance from the singular points to the center of the unit circle, is 0.075. The correspondence of points on the airfoil with those on the circle is plotted in figure 11, which shows the arc length of the airfoil as a function of the central angle of the circle. The velocity at any point on the airfoil for any angle of attack α_1 may be obtained from equations (A8) and (A9), using the velocity distribution as in figure 3(b) and the relation between s and θ as in figure 11. The ratio $\dfrac{\varphi'(s)}{v_{c,c}(\theta,\lambda)}$ is equal to $\dfrac{d\theta}{ds}$ (radians) and need be computed only once for any given airfoil.

APPENDIX B

DERIVATION OF THE CASCADE EQUATION

An equation is to be developed for the complex velocity at any point in the field of flow of a fluid past a row of equally spaced, congruent bodies. Coordinate axes are chosen with the origin inside one of the bodies and the x-axis in the direction of the row. (See fig. 12.) The body containing the origin is denoted by B_0, bodies along the positive direction of the x-axis by B_1, B_2, etc., and along the negative direction of the x-axis by B_{-1}, B_{-2}, etc. A circle A of small radius is drawn about the point z where the velocity is to be determined. A rectangle R is drawn with its center at the origin and its sides parallel to the axes of length $(2N+1)d$ and width $2t$, which contains the bodies $B_{-N} \cdots B_{-1}$, B_0, $B_1 \cdots B_N$, and the circle A. If a side of the rectangle intersects one of the bodies, the side may be distorted to go around the body with no essential change in the proof. The function $w(z_0)/z_0-z$ is an analytical function of z in the region inside the rectangle R but outside the bodies B_n and the circle A.

Therefore

$$\int_R \frac{w'(z_0)}{z_0-z}\,dz_0 - \int_A \frac{w'(z_0)}{z_0-z}\,dz_0 - \sum_{n=-N}^{N}\int_{B_n} \frac{w'(z_0)}{z_0-z}\,dz_0 = 0 \quad (B1)$$

The first integral can be broken up into four integrals, one along each side of the rectangle, namely,

$$\int_R \frac{w'(z_0)}{z_0-z}\,dz_0 = \int_{-(N+1/2)d}^{(N+1/2)d} \frac{w'(x_0-it)}{x_0-it-z}\,dx_0 + \int_{-t}^{t} \frac{w'[(N+1/2)d+iy_0]}{(N+1/2)d+iy_0-z}\,idy_0$$

$$+ \int_{(N+1/2)d}^{-(N+1/2)d} \frac{w'(x_0+it)}{x_0+it-z}\,dx_0 + \int_{t}^{-t} \frac{w'[-(N+1/2)d+iy_0]}{-(N+1/2)d+iy_0-z}\,idy_0$$

$$(B2)$$

In an evaluation of these integrals, the function $w'(z_0)$ is periodic, with period d, and approaches a constant value infinitely far from the cascade; that is,

$$w'(x_0 + iy_0) \rightarrow w_2' \text{ as } y_0 \rightarrow \infty$$

and

$$w'(x_0 + iy_0) \rightarrow w_1' \text{ as } y_0 \rightarrow -\infty$$

From the last of these conditions, it follows that

$$w'(x_0 - it) = w_3'(x_0 - it) + w_1'$$

where

$$w_3'(x_0 - it) \rightarrow 0 \text{ as } t \rightarrow \infty$$

Therefore, the first integral on the right side of equation (B2) is

$$\int_{-(N+1/2)d}^{(N+1/2)d} \frac{w'(x_0 - it)}{x_0 - it - z} dx_0 = w_1' \int_{-(N+1/2)d}^{(N+1/2)d} \frac{dx_0}{x_0 - it - z}$$

$$+ \int_{-(N+1/2)d}^{(N+1/2)d} \frac{w_3'(x_0 - it)}{x_0 - it - z} dx_0 \qquad (B3)$$

The first of these integrals is

$$w_1' \int_{-(N+1/2)d}^{(N+1/2)d} \frac{dx_0}{x_0 - it - z} = w_1' \log \frac{[(N+1/2)d - it - z]}{[-(N+1/2)d - it - z]} \rightarrow \pi i w_1'$$

as $N \rightarrow \infty$ and $t \rightarrow \infty$, provided that $\frac{t}{N} \rightarrow 0$. The last integral in equation (B3) is

$$\int_{-(N+1/2)d}^{(N+1/2)d} \frac{w_3'(x_0-it)}{x_0-it-z}\,dx_0 = \sum_{n=-N}^{N} \int_{(n-1/2)d}^{(n+1/2)d} \frac{w_3'(x_0-it)}{x_0-it-z}\,dx_0$$

$$= \sum_{n=-N}^{N} \int_{-1/2d}^{1/2d} \frac{w_3'(x_0-it)}{x_0+nd-it-z}\,dx_0$$

$$= \int_{-1/2d}^{1/2d} \frac{w_3'(x_0-it)}{x_0-it-z}\,dx_0 + \sum_{n=1}^{N} \int_{-1/2d}^{1/2d} \frac{2(x_0-it-z)w_3'(x_0-it)dx_0}{(x_0-it-z)^2 -n^2 d^2}$$

If t is chosen sufficiently large so that $\left|w_3'(x_0-it)\right| < \epsilon$, where ϵ is any preassigned positive number, the integrals are less than or equal to

$$\epsilon \left[\int_{-1/2d}^{1/2d} \frac{dx_0}{\left|x_0-it-z\right|} + \sum_{n=1}^{N} \int_{-1/2d}^{1/2d} \frac{2\left|x_0-it-z\right|\,dx_0}{\left|(x_0-it-z)^2 -n^2 d^2\right|} \right]$$

$$\stackrel{\leq}{=} \epsilon \left[\int_{-1/2d}^{1/2d} \frac{dx}{\sqrt{(x_0-x)^2+(y_0-t-y)^2}} + \sum_{n=1}^{N} \int_{-1/2d}^{1/2d} \frac{2\sqrt{(x_0-x)^2+(y_0-t-y)^2}dx_0}{(x_0-x)^2+(y_0-t-y)^2-n^2d^2} \right]$$

When $N \to \infty$, this quantity approaches

$$\epsilon \int_{-1/2d}^{1/2d} \frac{\pi}{d} \cot \frac{\pi}{d} \sqrt{(x_0-x)^2 + (y_0-t-y)^2}\,dx_0$$

This integral is finite and, because ϵ can be made arbitrarily small as $t \rightarrow \infty$, the last integral in equation (B3) approaches zero. Therefore,

$$\int_{-(N+1/2)d}^{(N+1/2)d} \frac{w'(x_o-it)}{x_o-it-z} dx_o \longrightarrow \pi i w_1'$$

as $N \rightarrow \infty$ and $t \rightarrow \infty$ while $\frac{t}{N} \rightarrow 0$. In the same way and under the same conditions,

$$\int_{(N+1/2)d}^{-(N+1/2)d} \frac{w'(x_o+it)}{x_o+it-z} dx_o \longrightarrow \pi i w_2'$$

The second and fourth integrals on the right side of equation (B2) can be evaluated by combining them. Because w' is periodic,

$$w'[(N+1/2)d+iy_o] = w'[-(N+1/2)d+iy_o]$$

and therefore,

$$\int_{-t}^{t} \frac{w'[(N+1/2)d+iy_o]}{(N+1/2)d+iy_o-z} i dy_o + \int_{t}^{-t} \frac{w'[-(N+1/2)d+iy_o]}{-(N+1/2)d+iy_o-z} i dy_o$$

$$= \int_{-t}^{t} \frac{-2(N+1/2)d \; w'[(N+1/2)d+iy_o]}{(iy_o-z)^2 - (N+1/2)^2 d^2} i dy_o$$

The velocity $w'[(N+1/2)d+iy_o]$ is bounded for all values of y_o; that is, there is a constant W such that $|w'[(N+1/2)d+iy_o]| < W$. The absolute value of the integral is less than

$$2d(N+1/2) \ W \int_{-t}^{t} \frac{dy_O}{\left| (iy_O-z)^2 \ - \ (N+1/2)^2 \ d^2 \right|}$$

$$\leqq 2d(N+1/2) \ W \int_{-t}^{t} \frac{dy_O}{(y_O-y)^2 \ + \ (N+1/2)^2 \ d^2-x^2}$$

$$= \frac{2d(N+1/2) \ W}{\sqrt{(N+1/2)^2 \ d^2-x^2}} \left[\tan^{-1} \frac{t-y}{\sqrt{(N+1/2)^2 \ d^2-x^2}} - \tan^{-1} \frac{-t-y}{\sqrt{(N+1/2)^2 \ d^2-x^2}} \right]$$

As $N \longrightarrow \infty$ and $t \longrightarrow \infty$, this quantity approaches zero. It has been shown, therefore, that when $t \longrightarrow \infty$ and $\frac{t}{N} \longrightarrow 0$,

$$\int_{R} \frac{w'(z_O)}{z_O-z} \ dz_O \longrightarrow \pi i \ (w_2'+ w_1') \tag{B4}$$

By the residue theorem,

$$\int_{A} \frac{w'(z_O)}{z_O-z} \ dz_O \ = 2\pi i w'(z) \tag{B5}$$

The periodicity of $w'(z)$ implies that

$$\sum_{n=-N}^{N} \int_{B_n} \frac{w'(z_o)}{z_o - z} \, dz_o = \sum_{n=-N}^{N} \int_{B_0} \frac{w'(z_o)}{z_o + nd - z} \, dz_o$$

$$= \int_{B_0} \frac{w'(z_o)}{z_o - z} \, dz_o + \sum_{n=1}^{N} \int_{B_0} \frac{w'(z_o) \, 2(z_o - z)}{(z_o - z)^2 - n^2 \, d^2} \, dz_o \longrightarrow \int_{B_0} \frac{\pi}{d} \, w'(z_o) \, \cot \frac{\pi}{d} \, (z_o - z) dz_o$$

$$(B6)$$

as $N \longrightarrow \infty$.

When equations (B4), (B5), and (B6) are substituted into equation (B1), the expression for the complex velocity is obtained:

$$w'(z) = \frac{1}{2}(w_1' + w_2') - \frac{1}{2\pi i} \int_{B_0} \frac{\pi}{d} \, w'(z_o) \, \cot \frac{\pi}{d} \, (z_o - z) \, dz_o$$

$$(B7)$$

The complex potential is obtained from equation (B7) by integrating with respect to z and neglecting the arbitrary constant,

$$w(z) = z \, w_m' + \frac{1}{2\pi i} \int_{B_0} w'(z_o) \, \log \sin \frac{\pi}{d} \, (z - z_o) \, dz_o \qquad (B8)$$

where $w_m' = \dfrac{w_1' + w_2'}{2}$ is the mean stream velocity.

APPENDIX C

SYMBOLS

The main symbols used throughout the report are listed here for convenience of reference.

d   distance between successive airfoils in cascade

$$f_1 \equiv \frac{1}{4\pi} \log \left[(x-x_0)^2 + (y-y_0)^2 \right]$$

$$f_2 \equiv \frac{1}{4\pi} \log \left[\sin^2 \frac{\pi}{d} (x-x_0) + \sinh^2 \frac{\pi}{d} (y-y_0) \right]$$

K   natural logarithm of distance from singular point to center of circle corresponding to cascade airfoils

l total arc length of airfoil

s   arc-length parameter corresponding to z

s_0 arc-length parameter correspondong to z_0

v_c local velocity on circle corresponding to isolated airfoil

$v_{c,c}$ local velocity on circle corresponding to airfoil in cascade

v_x velocity induced by vortices in region $f_2 > 0$

V   magnitude of uniform or mean stream velocity in airfoil or cascade plane (fig. 1)

V_c magnitude of uniform stream velocity in circle plane

V_x x-component of uniform or mean stream velocity V

$V_{x,r}$ resultant local mean stream x-component of velocity V

V_y y-component of uniform or mean stream velocity V

w   complex potential function, $(\varphi + i\psi)$

w_u' complex velocity of uniform stream for isolated airfoil, $(V_x - iV_y)$

$w_m{}'$ complex velocity of mean stream for airfoil in cascade
$$\left(w_m{}' = \frac{1}{2}(w_1{}' + w_2{}') = V_x - iV_y\right)$$

x_c, y_c coordinates of point about which airfoil is rotated (centroid of vortex distribution for cascade airfoils)

z coordinate of point where stream function is computed, $(x + iy)$

z_0 coordinate of point where vortex is located, $(x_0 + iy_0)$

α angle of inclination of uniform stream velocity to x-axis

β angle through which airfoil is rotated

$\gamma(z_0)$ vortex strength per unit arc length at z_0

Γ circulation about airfoil

θ central angle of circle

θ_N angle of stagnation point on circle corresponding to leading edge of airfoil

θ_T angle of stagnation point on circle corresponding to trailing edge of airfoil

λ angle of inclination of mean flow to normal to cascade axis (fig. 1)

φ velocity potential on airfoil, $R[w(z)]$

φ_c velocity potential on circle corresponding to isolated airfoil

$\varphi_{c,c}$ velocity potential on circle corresponding to airfoil in cascade

$\varphi_A, \varphi_B,$ values of φ at points A, B, C, D, respectively, where
φ_C, φ_D the curve of $\varphi(s_0)$ intersects $f_2(s, s_0) = 0$ (See figure 5.)

φ_{min} velocity potential at the leading edge of the airfoil

ψ stream function, $I[w(z)]$

ψ_m stream function of mean stream of cascade flow

ψ_u stream function of uniform stream flowing about isolated
          airfoil

$\overline{\psi}$ mean value of stream function over airfoil

$\Delta\psi$ variation of stream function, $(\psi - \overline{\psi})$

Subscripts 1 and 2 when appended to w', V, and V_x indicate entrance
and discharge values, respectively.

REFERENCES

1. Mutterperl, William: The Conformal Transformation of an Airfoil
   into a Straight Line and Its Application to the Inverse Problem
   of Airfoil Theory. NACA ARR No. L4K22a, 1944.

2. Theodorsen, Theodore: Airfoil-Contour Modifications Based on
   ϵ-Curve Method of Calculating Pressure Distribution. NACA
   ARR No. L4G05, 1944.

3. Mutterperl, William: A Solution of the Direct and Inverse
   Potential Problems for Arbitrary Cascades of Airfoils. NACA
   ARR No. L4K22b, 1944.

4. Ackeret, J.: The Design of Closely Spaced Blade Grids. British
   R.T.P. Trans. No. 2007, Ministry Aircraft Prod. (From Schweiz.
   Bauzeitung, vol. 120, no. 9, Aug. 29, 1942, pp. 103-108.)

5. von Mises, Richard, and Friedrichs, Kurt O.: Fluid Dynamics,
   Advance Instruction and Research in Mechanics, ch. III.
   Brown Univ., Summer, 1941, pp. 96-97.

6. Stodola, A.: Steam and Gas Turbines. Vol. II. McGraw-Hill
   Book Co., Inc., 1927, pp. 992-994. (Reprinted, Peter Smith
   (New York), 1945.)

7. von Kármán, Th.: Compressibility Effects in Aerodynamics.
   Jour. Aero. Sci., vol. 8, no. 9, July 1941, pp. 337-356.

8. Garrick, I. E., and Kaplan, Carl: On the Flow of a Compressible
   Fluid by the Hodograph Method. I - Unification and Extension
   of Present-Day Results. NACA ACR No. L4C24, 1944.

9. Theodorsen, T., and Garrick, I. E.: General Potential Theory of
     Arbitrary Wing Sections. NACA Rep. No. 452, 1933.

10. Garrick, I. E.: On the Plane Potential Flow past a Symmetrical
     Lattice of Arbitrary Airfoils. NACA ARR No. 4A07, 1944.

11. Gebelein, H.: Theory of Two-Dimensional Potential Flow about
     Arbitrary Wing Sections. NACA TM No. 886, 1939.

TABLE I.   COORDINATES OF $f_2(x-x_0, y-y_0)$

(a)   Values of $\dfrac{y-y_0}{d}$

NATIONAL ADVISORY
COMMITTEE FOR AERONAUTICS

$\dfrac{x-x_0}{d}$ / f_2	0	0.05	0.10	0.15	0.20	0.25	0.30	0.35	0.40	0.45	0.50
−0.40	0.0257	−	−	−	−	−	−	−	−	−	−
−.38	.0292	−	−	−	−	−	−	−	−	−	−
−.36	.0331	−	−	−	−	−	−	−	−	−	−
−.34	.0375	−	−	−	−	−	−	−	−	−	−
−.32	.0425	−	−	−	−	−	−	−	−	−	−
−.30	.0481	−	−	−	−	−	−	−	−	−	−
−.28	.0545	0.0229	−	−	−	−	−	−	−	−	−
−.26	.0618	.0371	−	−	−	−	−	−	−	−	−
−.24	.0699	.0497	−	−	−	−	−	−	−	−	−
−.22	.0791	.0621	−	−	−	−	−	−	−	−	−
−.20	.0894	.0750	−	−	−	−	−	−	−	−	−
−.18	.1010	.0887	0.0296	−	−	−	−	−	−	−	−
−.16	.1140	.1035	.0620	−	−	−	−	−	−	−	−
−.14	.1286	.1195	.0871	−	−	−	−	−	−	−	−
−.12	.1447	.1369	.1107	0.0392	−	−	−	−	−	−	−
−.10	.1626	.1560	.1344	.0881	−	−	−	−	−	−	−
−.08	.1824	.1768	.1588	.1241	0.0454	−	−	−	−	−	−
−.06	.2041	.1993	.1844	.1572	.1103	−	−	−	−	−	−
−.04	.2277	.2236	.2113	.1896	.1558	0.1014	−	−	−	−	−
−.02	.2532	.2498	.2396	.2222	.1966	.1608	0.1096	−	−	−	−
0	.2805	.2778	.2694	.2553	.2354	.2096	.1777	0.1400	0.0969	0.0496	0.0000
.02	.3097	.3074	.3006	.2892	.2737	.2542	.2318	.2081	.1858	.1692	.1629
.04	.3405	.3386	.3331	.3239	.3117	.2968	.2804	.2638	.2491	.2389	.2352
.06	.3728	.3713	.3668	.3595	.3498	.3384	.3260	.3139	.3036	.2965	.2940
.08	.4064	.4052	.4016	.3958	.3881	.3793	.3698	.3608	.3533	.3482	.3464
.10	.4412	.4402	.4373	.4327	.4267	.4198	.4126	.4058	.4001	.3964	.3951
.12	.4769	.4761	.4739	.4702	.4655	.4601	.4545	.4493	.4451	.4423	.4413
.14	.5135	.5129	.5111	.5082	.5045	.5003	.4960	.4920	.4888	.4867	.4859
.16	.5508	.5503	.5488	.5466	.5437	.5404	.5371	.5340	.5316	.5299	.5294
.18	.5886	.5882	.5871	.5853	.5830	.5805	.5779	.5755	.5736	.5724	.5720
.20	.6269	.6266	.6257	.6243	.6225	.6205	.6185	.6167	.6152	.6143	.6140
.22	.6655	.6653	.6646	.6635	.6621	.6606	.6590	.6576	.6565	.6557	.6555
.24	.7044	.7042	.7037	.7029	.7018	.7006	.6994	.6983	.6974	.6968	.6966

TABLE I. COORDINATES OF $f_2(x-x_0, y-y_0)$ – CONTINUED.

(a) Values of $\dfrac{y-y_0}{d}$ – Concluded.

$\dfrac{x-x_0}{d}$ / f_2	0	0.05	0.10	0.15	0.20	0.25	0.30	0.35	0.40	0.45	0.50
0.26	0.7436	0.7434	0.7430	0.7424	0.7415	0.7406	0.7396	0.7388	0.7381	0.7377	0.7375
.28	.7829	.7828	.7825	.7820	.7813	.7806	.7798	.7792	.7787	.7783	.7782
.30	.8224	.8223	.8221	.8217	.8211	.8206	.8200	.8195	.8191	.8188	.8187
.32	.8620	.8619	.8617	.8614	.8610	.8606	.8601	.8597	.8594	.8592	.8592
.34	.9017	.9016	.9015	.9012	.9009	.9006	.9002	.8999	.8997	.8995	.8995
.36	.9415	.9414	.9413	.9411	.9409	.9406	.9403	.9401	.9399	.9398	.9397
.38	.9813	.9812	.9811	.9810	.9808	.9806	.9804	.9802	.9800	.9800	.9799
.40	1.0211	1.0211	1.0210	1.0209	1.0207	1.0206	1.0204	1.0203	1.0201	1.0201	1.0201
.42	1.0610	1.0610	1.0609	1.0608	1.0607	1.0606	1.0604	1.0603	1.0602	1.0602	1.0602
.44	1.1009	1.1009	1.1008	1.1008	1.1007	1.1006	1.1005	1.1004	1.1003	1.1003	1.1003
.46	1.1408	1.1408	1.1408	1.1407	1.1407	1.1406	1.1405	1.1404	1.1404	1.1403	1.1403
.48	1.1808	1.1807	1.1807	1.1807	1.1806	1.1806	1.1805	1.1805	1.1804	1.1804	1.1804
.50	1.2207	1.2207	1.2207	1.2206	1.2206	1.2206	1.2205	1.2205	1.2204	1.2204	1.2204
.52	1.2607	1.2607	1.2607	1.2606	1.2606	1.2606	1.2605	1.2605	1.2605	1.2605	1.2605
.54	1.3007	1.3006	1.3006	1.3006	1.3006	1.3006	1.3005	1.3005	1.3005	1.3005	1.3005
.56	1.3406	1.3406	1.3406	1.3406	1.3406	1.3406	1.3405	1.3405	1.3405	1.3405	1.3405
.58	1.3806	1.3806	1.3806	1.3806	1.3806	1.3806	1.3805	1.3805	1.3805	1.3805	1.3805
.60	1.4206	1.4206	1.4206	1.4206	1.4206	1.4206	1.4205	1.4205	1.4205	1.4205	1.4205
.62	1.4606	1.4606	1.4606	1.4606	1.4606	1.4606	1.4605	1.4605	1.4605	1.4605	1.4605
.64	1.5006	1.5006	1.5006	1.5006	1.5006	1.5006	1.5005	1.5005	1.5005	1.5005	1.5005
.66	1.5406	1.5406	1.5406	1.5406	1.5406	1.5406	1.5406	1.5405	1.5405	1.5405	1.5405
.68	1.5806	1.5806	1.5806	1.5806	1.5806	1.5806	1.5806	1.5805	1.5805	1.5805	1.5805
.70	1.6206	1.6206	1.6206	1.6206	1.6206	1.6206	1.6206	1.6205	1.6205	1.6205	1.6205

TABLE I.   COORDINATES OF $f_2(x-x_0, y-y_0)$ — CONCLUDED.

(b)   Values of $\dfrac{x-x_0}{d}$

$\dfrac{y-y_0}{d}$ / f_2	0	0.025	0.050	0.075	0.100	0.125	0.150	0.175	0.200	0.225	0.250
-0.40	0.0258	0.0060	-	-	-	-	-	-	-	-	-
-.38	.0293	.0151	-	-	-	-	-	-	-	-	-
-.36	.0332	.0217	-	-	-	-	-	-	-	-	-
-.34	.0377	.0281	-	-	-	-	-	-	-	-	-
-.32	.0428	.0346	-	-	-	-	-	-	-	-	-
-.30	.0485	.0414	-	-	-	-	-	-	-	-	-
-.28	.0551	.0489	0.0219	-	-	-	-	-	-	-	-
-.26	.0625	.0572	.0367	-	-	-	-	-	-	-	-
-.24	.0710	.0663	.0496	-	-	-	-	-	-	-	-
-.22	.0808	.0766	.0625	0.0256	-	-	-	-	-	-	-
-.20	.0918	.0882	.0761	.0500	-	-	-	-	-	-	-
-.18	.1046	.1013	.0908	.0700	0.0148	-	-	-	-	-	-
-.16	.1192	.1163	.1071	.0897	.0571	-	-	-	-	-	-
-.14	.1362	.1336	.1254	.1105	.0854	0.0317	-	-	-	-	-
-.12	.1559	.1535	.1462	.1330	.1123	.0782	-	-	-	-	-
-.10	.1791	.1769	.1702	.1585	.1405	.1137	0.0685	-	-	-	-
-.08	.2068	.2047	.1985	.1877	.1717	.1490	.1160	0.0572	-	-	-
-.06	.2406	.2386	.2326	.2225	.2076	.1873	.1598	.1204	0.0463	-	-
-.04	.2837	.2816	.2756	.2654	.2509	.2317	.2068	.1743	.1290	0.0408	-
-.02	.3437	.3414	.3344	.3229	.3072	.2871	.2624	.2321	.1942	.1432	0.0487

Fig. 1

NATIONAL ADVISORY
COMMITTEE FOR AERONAUTICS

Exit velocity diagram

Entrance velocity diagram

Complete velocity diagram

Reflected velocity diagram
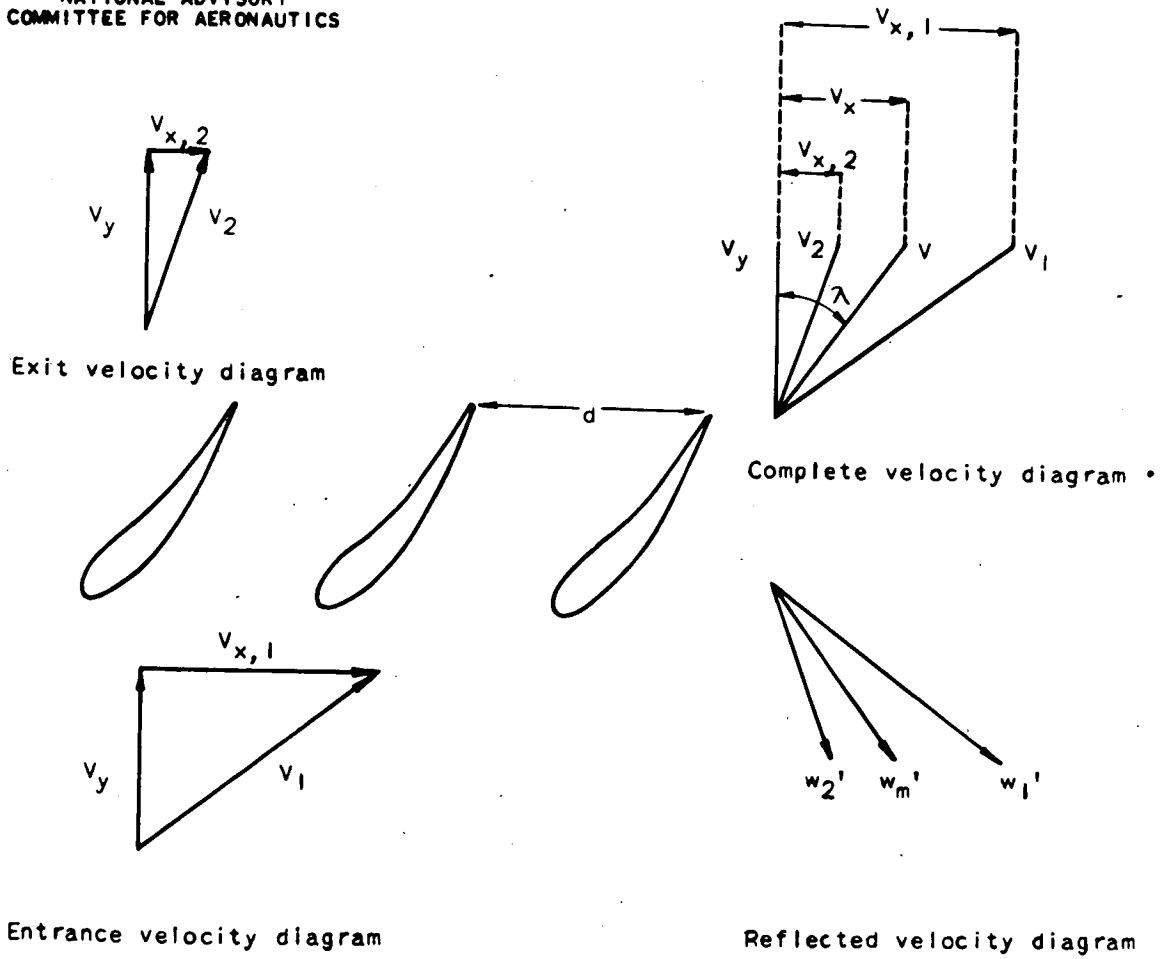
Figure 1. — Notation for cascade flow.

Fig. 2   NACA TN No. 1308

NATIONAL ADVISORY
COMMITTEE FOR AERONAUTICS
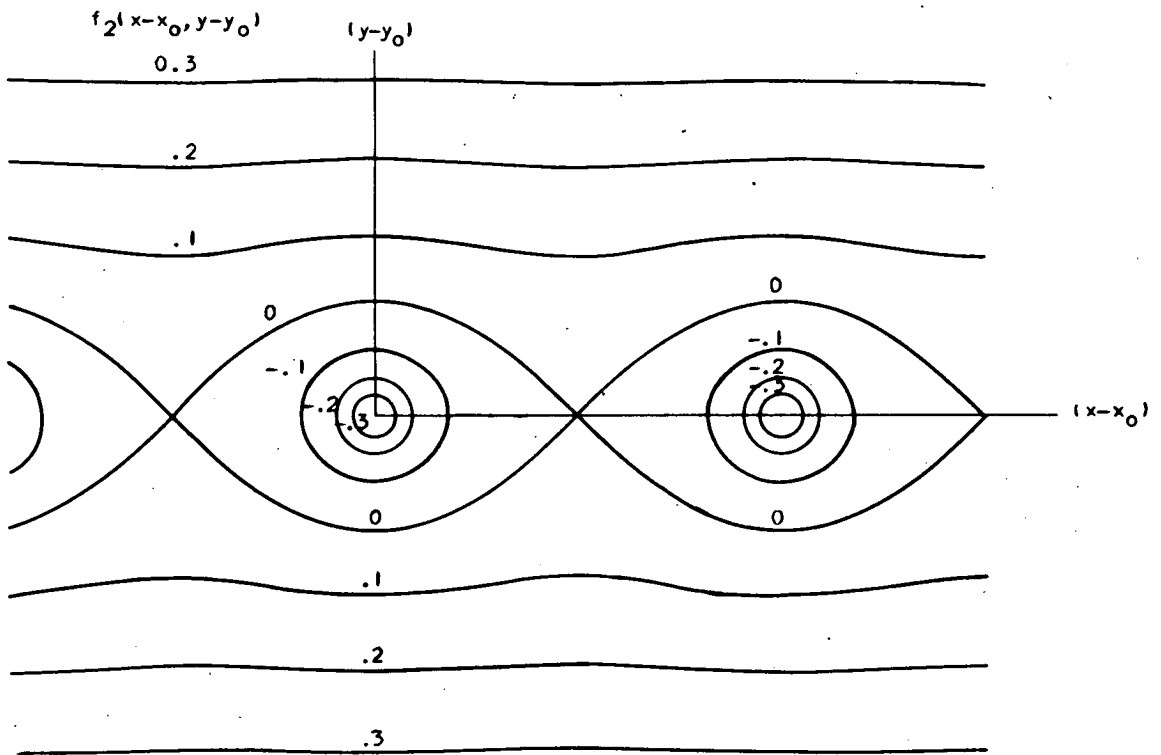
Figure 2. – Plot of curves for constant $f_2(x-x_0, y-y_0)$.

Figure 3. - Prescribed velocity distribution for thick airfoil in cascade.
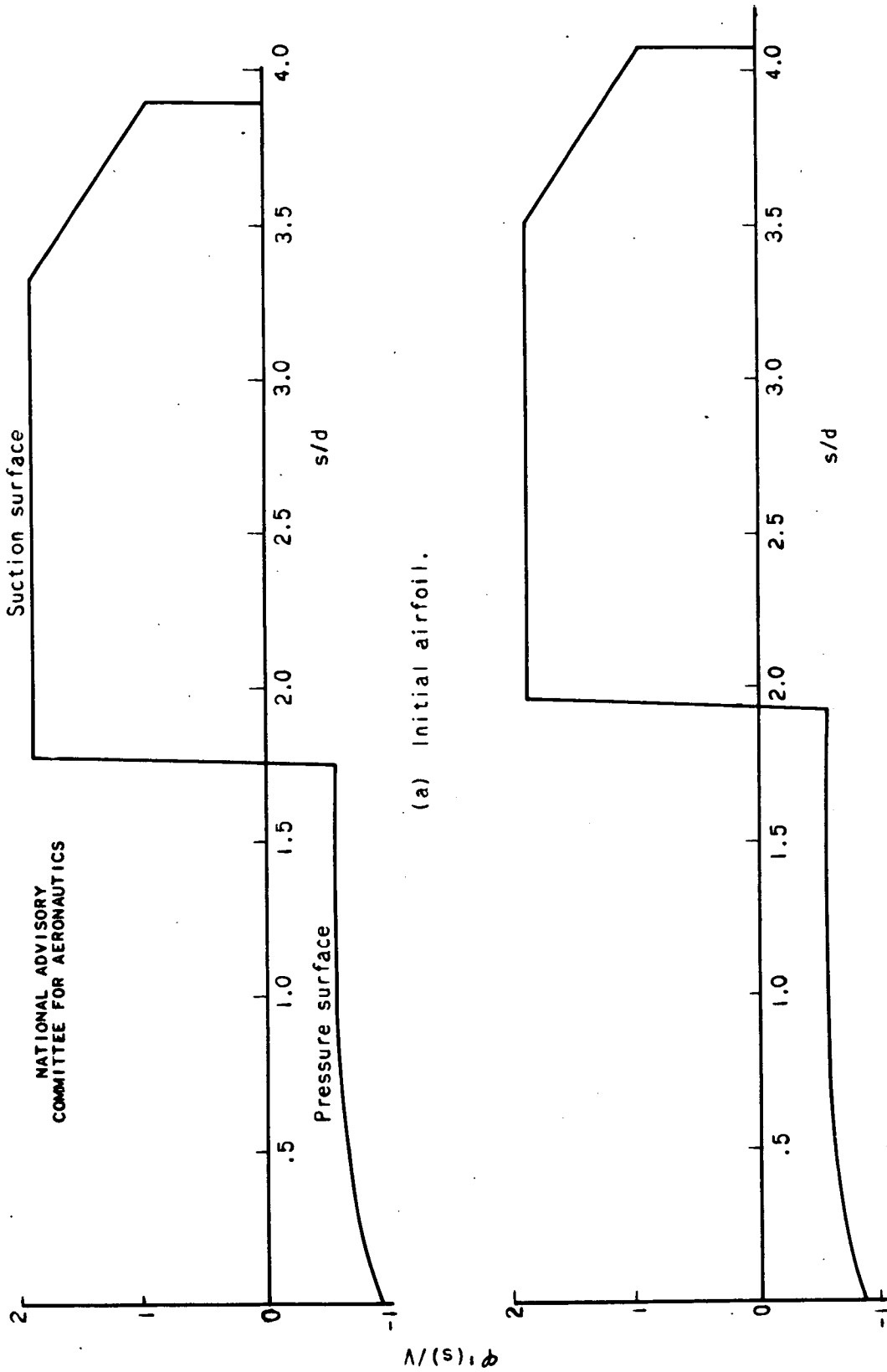
(a) Initial airfoil.

(b) Final airfoil.

Fig. 4   NACA TN No. 1308
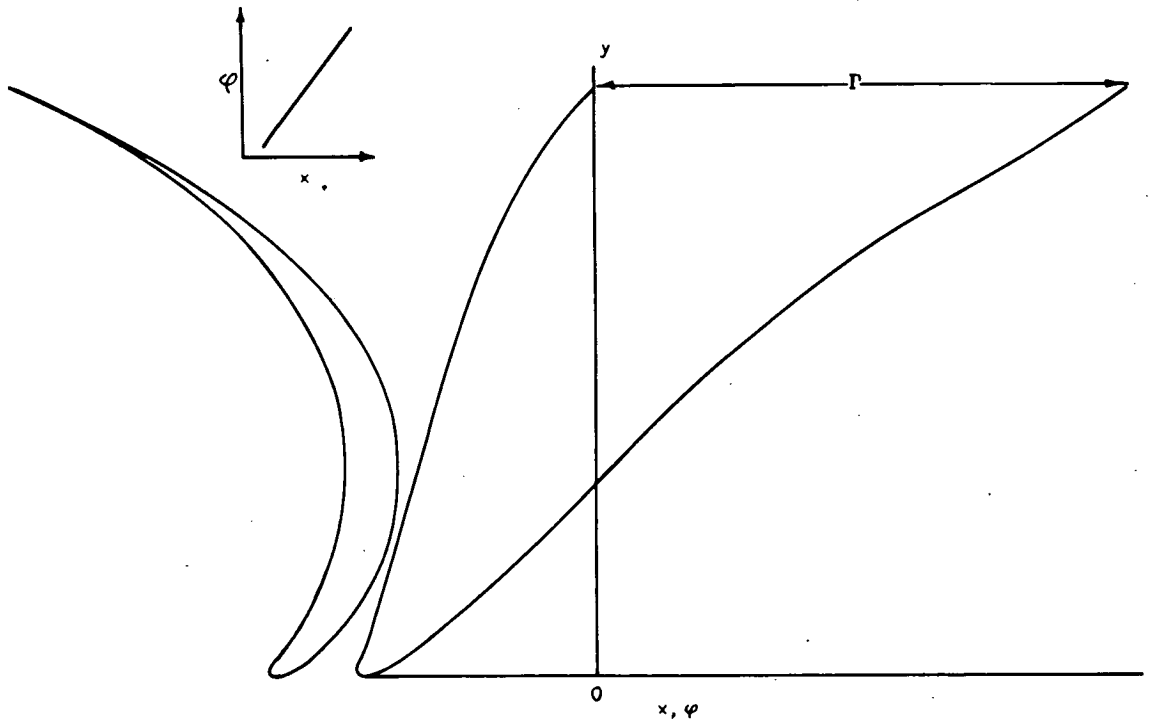
Figure 4. - Plot of airfoil and velocity potential for use in computation.

NATIONAL ADVISORY
COMMITTEE FOR AERONAUTICS

Figure 5. – Superposition of figures 2 and 4 to obtain plot of f_2 against φ.

Fig. 6   NACA TN No. 1308
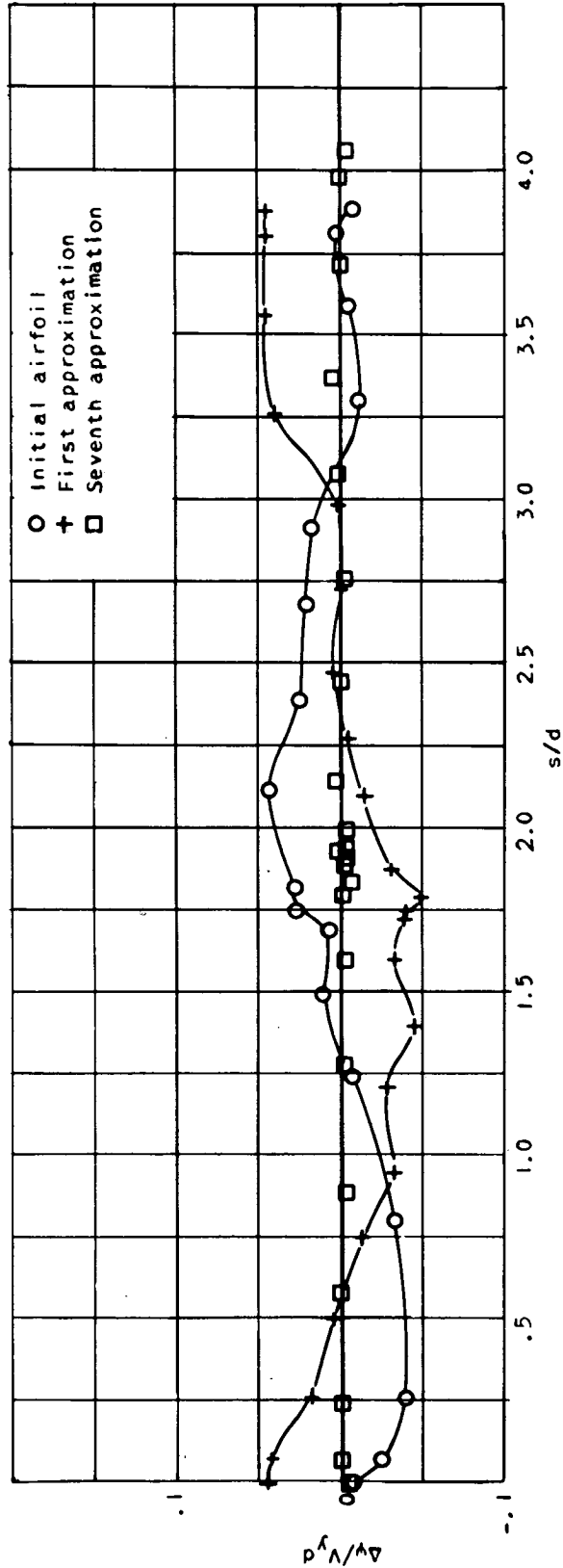
Figure 6. - Variation in stream function along initial shape and first and seventh approximations of airfoil cascade.
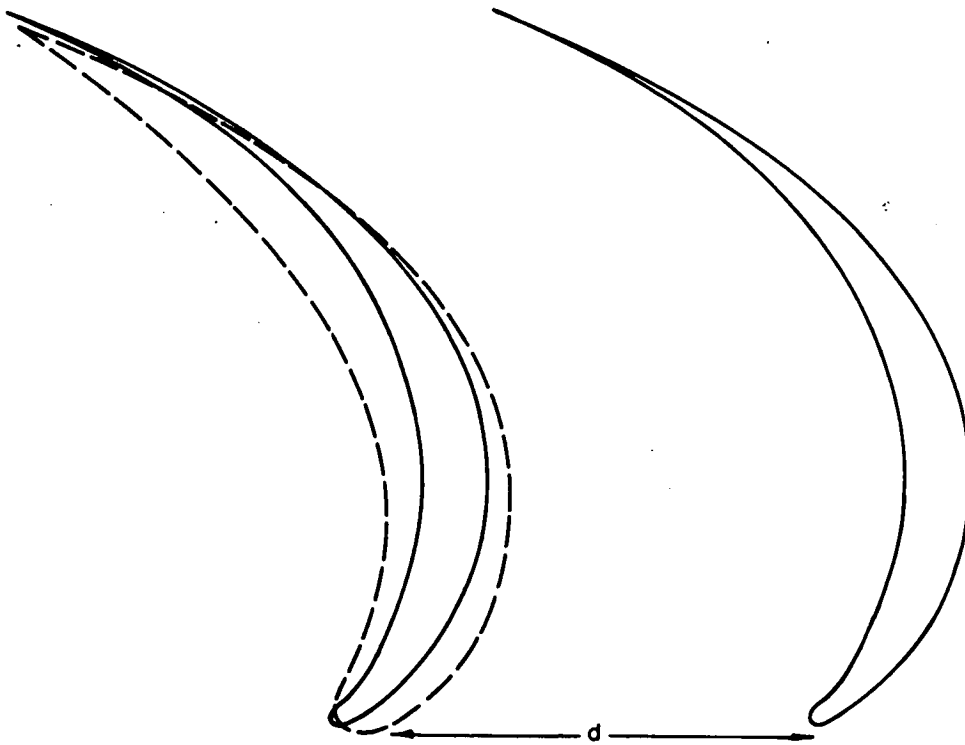
Figure 7. – Initial shape and final approximation of thick air-
foil showing cascade spacing.

Fig. 8   NACA TN No. 1308
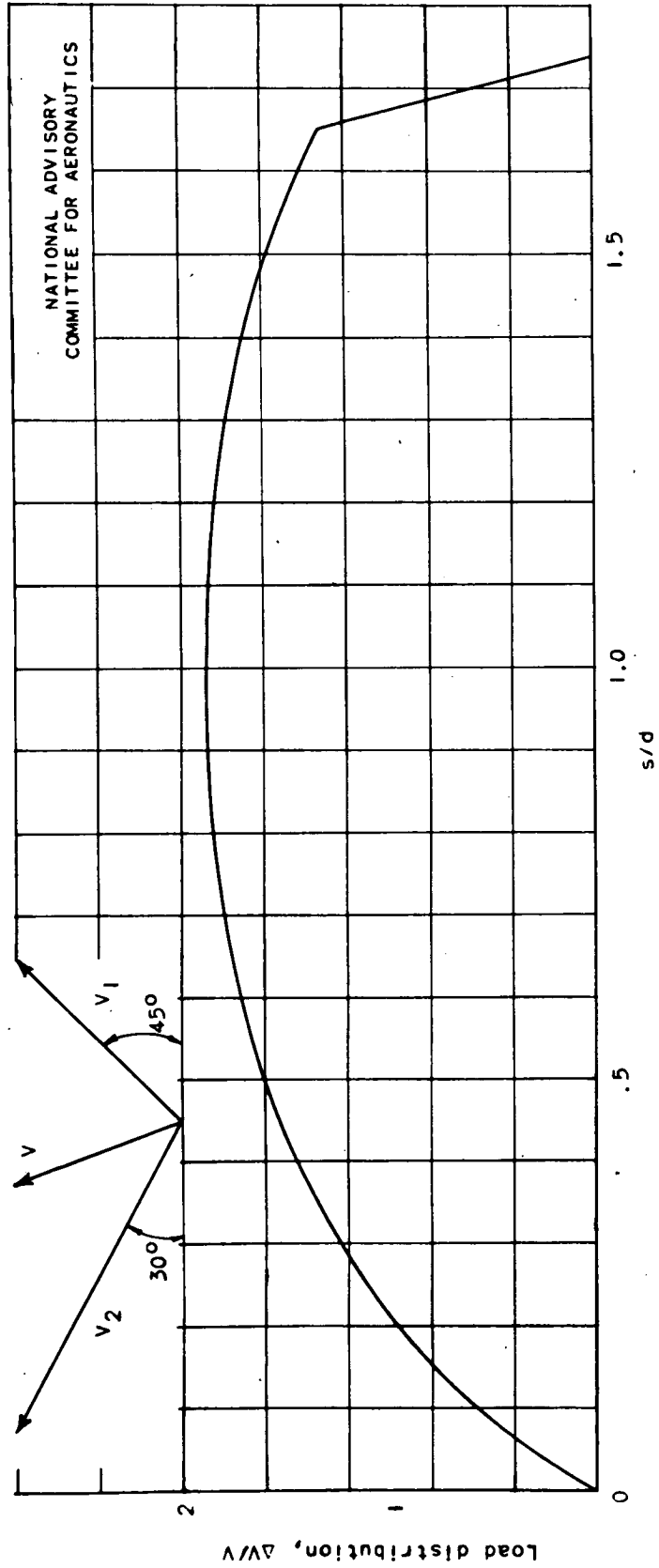
Figure 8. - Velocity diagram and prescribed load distribution for thin airfoil in cascade.

— — — — — Initial airfoil
— — — First approximation
——————— Third approximation

d
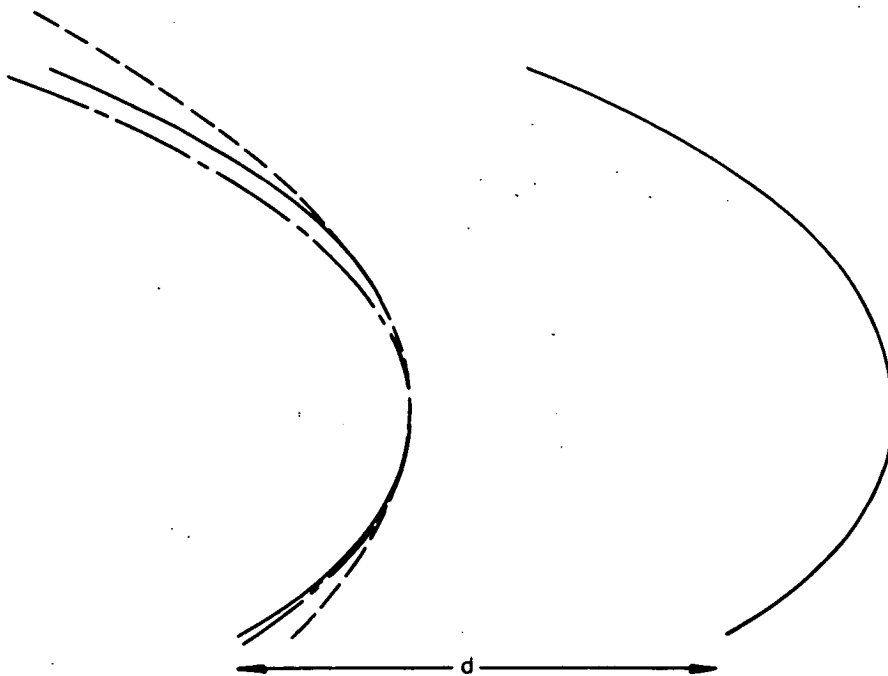
Figure 9. – Assumed shape and first and third approximations
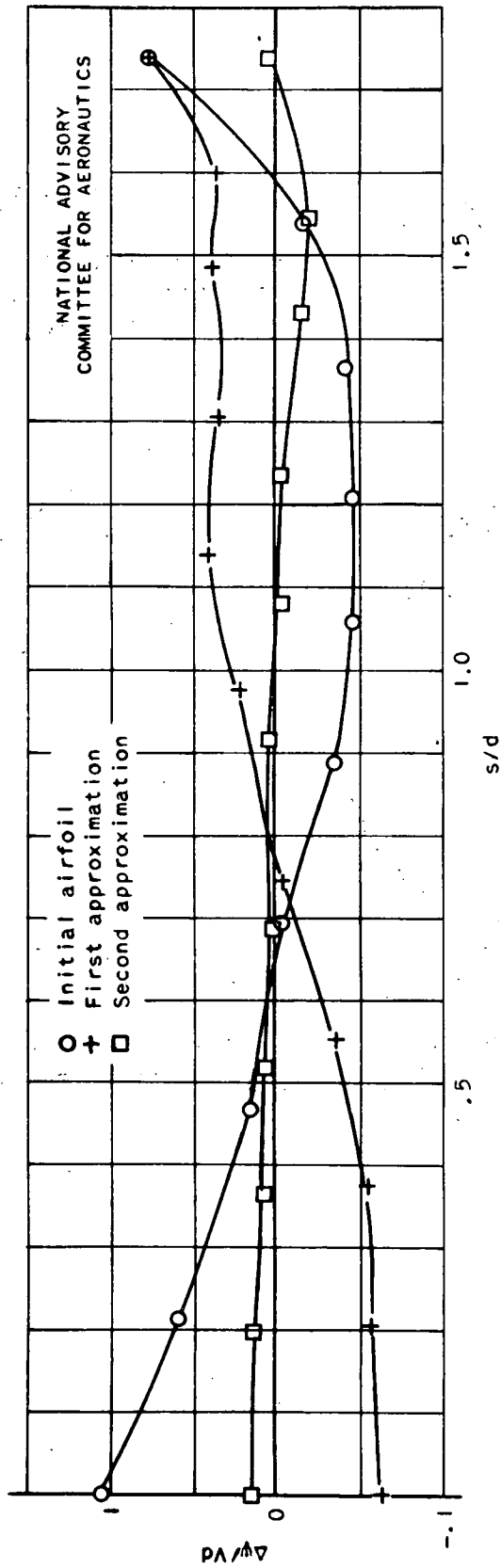of thin airfoil showing cascade spacing.

Fig. 10   NACA TN No. 1308

Figure 10. – Variation in stream function for successive approximation of thin airfoil in cascade.

Fig. II
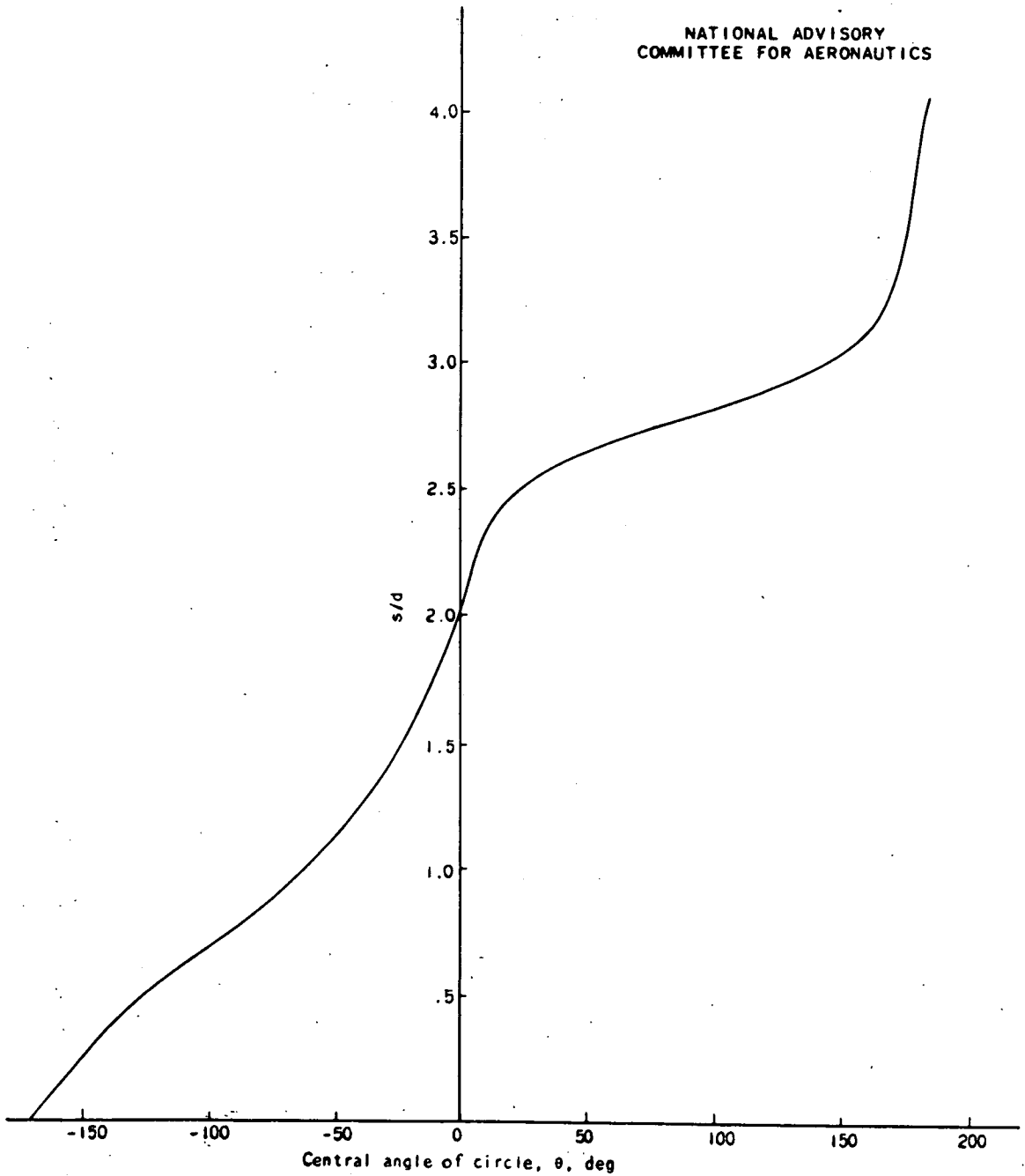
Figure II. - Correspondence between points on airfoil and points on unit circle
by conformal transformation.

Fig. 12   NACA TN No. 1308
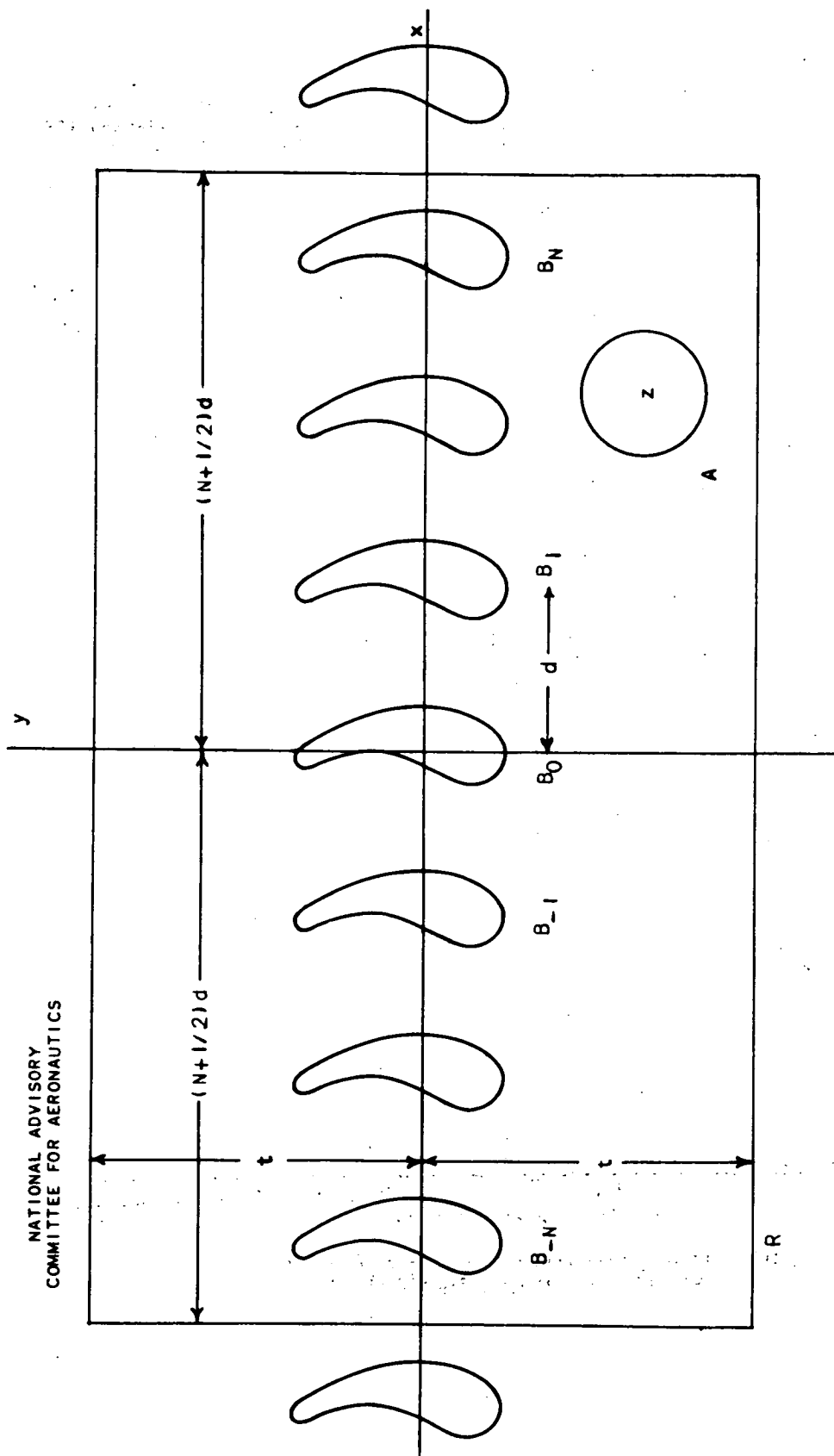
Figure 12. – Diagram for derivation of equation of flow about cascade.